Multi-omics analyses unveil the molecular mechanism involving significant bioactive substances of sea buckthorn at various growth years

Lichao He
Inner Mongolia Agricultural University
Meng Li
Arxan Forest Industry Co., Ltd
Xuewei Shi
Inner Mongolia Agricultural University
A Ruhan
Inner Mongolia Agricultural University
Gentu Ge
Inner Mongolia Agricultural University
Yanzi Xiao
Hulunbuir University
Yushan Jia
Inner Mongolia Agricultural University
Shuai Du
dushuai_nm@sina.com

Inner Mongolia Agricultural University

Article

Keywords: Hippophae rhamnoides L., Tree age, Source-sink synergy, Bioactive substances, Multi-omics analysis

Posted Date: May 30th, 2026

DOI: https://doi.org/10.21203/rs.3.rs-9752587/v1

Additional Declarations: No competing interests reported.

Abstract

The present work seeks to elucidate the source-sink coordination linking the shoots and berries of sea buckthorn (*Hippophae rhamnoides* L.) growth for 4, 5 and 6 years (4 year, 5 year and 6 year) based on integrated phenotypic and multi-omics analyses. Results indicated that with the increasing of tree age, a significant “two-stage” functional remodeling was undergone by the branches (the source). During the 4 year – 5 year period, driven by *PRKAA* and *PP2C*, the branches were primarily dedicated to reserving energy and glycosyl donors while suppressing efflux activities. Subsequently, during the 5 year – 6 year period, facilitated by the activation of *MYBP* and *PIP5K*, a comprehensive shift toward the targeted transport of metabolites was executed. The potential of source-end transcriptional activities to regulate sink-end correlational evidence substantiated the metabolite enrichment between branch genes and fruit metabolites. Furthermore, the weight and redness of the fruits (the sink) were significantly enhanced, and their core flavonoid metabolic strategy evolved from monomer accumulation to the synthesis of highly stable glycosidic compounds. In conclusion, the critical role of the branches as a key factor driving fruit quality development was elucidated in this study, thereby providing a solid research foundation for the age-appropriate harvesting and source-sink theory-based directional cultivation of sea buckthorn.

INTRODUCTION

As a dual-purpose woody species of significant ecological and its economic value, the sea buckthorn (*Hippophae rhamnoides* L.) possesses abundant repertoire of biologically active substances portrait flavonoids, carotenoids, Vitamin C and phenolic compounds acids within its berries. A pronounced potential for application has been exhibited by this species across the functional food and biomedical sectors[1–3]. Crucially, the precise regulation of flavonoid glycoside ratios by tree age is suggested to supply a critical scientific foundation for the timed harvesting of sea buckthorn. This targeted approach potentially facilitates the development of high-stability functional beverages, precision-targeted dietary supplements, and natural colorants with enhanced shelf-life[4].The visual color and secondary metabolite profiles are considered core indicators for quality evaluation, and their accumulation is closely associated with physiological states, including tree age[5]. Elucidating these mechanisms is therefore of paramount importance for guiding the directional enrichment of functional components and maximizing maximizing the market potential of sea buckthorn-based goods.

Lately, a wealth of scholarly investigations focusing on the mechanisms of fruit development and metabolites accumulation in the sea buckthorn have been conducted by researchers worldwide. Regarding the dissection of metabolic networks, it has been demonstrated that the internal flavonoid and phenylpropanoid metabolic pathways of the sea buckthorn undergo profound transcriptional and metabolic reprogramming at various growth and developmental stages, by which the precipitation of fruit pigments and antioxidant activities are directly affected[4, 6]. Furthermore, within the realm of woody plant physiology, the source-sink coordination between the branches and fruits is recognized as a pivotal

mechanism driving fruit development[7]. It has been confirmed that the cross-tissue Transport of secondary metabolites (such as flavonoids) and glycoside derivatives, is highly dependent on the synergistic involvement of transmembrane proteins, including the ABC transporters, and substrate mobilization pathways[8]. However, existing research has predominantly been confined to the compositional analysis of individual the sea buckthorn tissues (either fruits or branches)[9, 10]. Preliminary explorations are still lacking of regarding the molecular mechanisms by which the sea buckthorn branches act as the “source” to regulate the metabolic flux under different tree ages, and how this cross-tissue “source-sink” translocation drives the color evolution and glycosylation remodeling at the fruit “sink” end.

It has been proved by previous studies that the sea buckthorn reaches its most vigorous growth phase during the fifth year[11]. This crucial period not only enhances the development of the branches but also significantly influences the fruit's nutrient allocation and the accumulation of valuable bioactive compounds. In light of this, the branches and fruits of the sea buckthorn after continuous growth for 4, 5 and 6 years (4 year, 5 year and 6 year) were selected as the research subjects. In the current study, the phenotypic analysis, along with targeted/comprehensive metabolomic screening alongside large-scale RNA-Seq analysis technologies were integrated to dissect the dynamic evolution of nutrient allocation and metabolite accumulation between the branches and fruits driven by the tree age. Ultimately, from a “source-sink” perspective, a solid scientific foundation is provided for the directional Cultivation of Sea Buckthorn and the efficient extraction of its core bioactive compounds.

MATERIALS AND METHODS

Raw Material Acquisition

The branches and fruits of the sea buckthorn (*Hippophae rhamnoides* L.) across three growth ages (4 year, 5 year, and 6 year) were harvested on October 26, 2025, at the sea buckthorn plantation in the Aershan, Xing'an, Inner Mongolia, China. Samples of the same cultivar (Cultivar: *Hippophae rhamnoides* ‘Shenqiuhong’) from different growth years were collected. Subsequently, the fruits and branches were manually separated, and various indicators were determined for each tissue separately.

Determination of Apparent Indicators and Vitamin C Contents of the Sea Buckthorn Fruits

The color indicators (L*, a* and b*) of the sea buckthorn fruits were primarily measured using a colorimeter (YS3010 Shenzhen ThreeNH Technology Co., Ltd., Shenzhen, China) according to the previous method[12]. Fruit morphological parameters (length, width, and height) were ascertained via a digital caliper (CD-15APX, Mitutoyo Corp., Kawasaki, Japan). Furthermore, ascorbic acid levels were quantified employing the 2,6-dichloroindophenol titrimetric technique[13].

Individual stock solutions of anthocyanin standards were formulated at 10 mg · mL^{-1}

by precisely weighing each compound followed by dissolution in pure methanol. Appropriate volumes of these stock solutions were mixed to prepare a mixed standard a working series calibrated at 100 μg/mL, which was stored for further use. Instrumental analysis was performed according to the concentration gradients detailed in the Table S4. Samples were ultrasonically extracted with acidified hydromethanol (70:30:1 v/v/v methanol: water: formic acid) for 20 min, followed by clarificatory centrifugation (12,000 rpm, 10 min). The supernatant was collected and purified utilizing an HLB-SPE cartridge, the stationary phase underwent initial conditioning with absolute methanol and deionized water, followed by an aqueous rinse and final elution via 5% formic acid in methanol. Target analytes were concentrated by evaporating the eluent under N_2 gas and freeze-drying, followed by redissolution in 0.2 mL of methanol. Subsequent centrifugal clarification provided the supernatant for downstream injection.

The required standard compounds of carotenoids were accurately weighed and dissolved in acetone to prepare individual stock solutions at a concentration of 200 μg/mL. Appropriate volumes of these stock solutions were mixed to prepare mixed standard solutions at concentrations of 17.5 μg/mL, 14 μg/mL, and 7 μg/mL, which were stored for further use. Instrumental analysis was performed according to the concentration gradients detailed in the Table S5. Samples were treated with anhydrous ethanol supplemented with 0.1% BHT (2,6-di-tert-butyl-4-methylphenol) and an 80% (w/v) KOH aqueous solution to facilitate saponification in an 80°C water bath. Subsequently, hexane and ultrapure water were added for vortex extraction twice centrifugal separation at 3,000 rpm for 5 min. Integrated supernatants underwent solvent removal via N_2 blow-down at 30°C, the obtained extract was then reconstituted into 0.2 mL of MeOH for final analysis.

Sample Extraction and Pretreatment: Anthocyanins: Carotenoids:

Chromatographic separation was performed using a Vanquish UPLC platform (Thermo Fisher Scientific, USA) equipped with a Waters HSS T3 column (50×2.1 mm, 1.8 μm), maintained at a stable 40°C. Samples were held at 4°C in the autosampler, with 2 μl aliquots injected for analysis. The mobile phase consisted of 0.1% formic acid in water (A) and acetonitrile (B). At a constant flow of 0.3mL/min, the gradient was programmed as: 0–1 min, 5% B, 6 min, 30% B, 7–8 min, 95% B, and 8.1–10 min, 5% B. Mass detection was executed via a Q Exactive high-resolution system (Thermo Fisher Scientific) utilizing an ESI source in positive SIM mode (scan range: m/z 200–700)."Carotenoid detection system: A dual ternary DGLC ultra-high performance liquid chromatography system equipped with a DAD detector (Thermo Fisher Scientific, USA) was utilized, featuring a YMC Carotenoid S-3 μm column (150 × 4.6 mm). Carotenoid monitoring was conducted at a fixed wavelength of 450 nm. The binary mobile phase utilized pure methanol (A) and a ternary mixture of methanol, methyltert-butyl ether, and H2O (20:75:5, v/v/v) (B). Chromatographic elution proceeded at 1.0 mL/min using the following linear gradient: 0% B at 0 min,

reaching 61% B by 15 min, escalating to 100% B at 25 min, and re-equilibrating to 0% B from 25.1 to 30 min.

Quantitative Analysis and Quality Control (QC) of data were processed using the TraceFinder software (for anthocyanins) and Chromeleon 7 software (for carotenoids) for baseline filtering and peak identification. Absolute quantification was performed utilizing an external standard curve method. To monitor system stability, samples were injected in a randomized order throughout the entire detection process, and an equal-volume mixture of QC samples was inserted after every 20 samples. System stability and data reliability were evaluated based on the RSD values (precision index) (RSD < 30%) of the peak areas of the targeted compounds in the QC samples.

Untargeted Metabolomics Analysis of the Sea Buckthorn Fruits and Branches

Untargeted metabolomics analysis was performed on a total of 60 fruit and branch samples in this study. Following sampling, 0.05 g of the tissue sample was placed into 400 μL of an 80% aqueous methanol solution containing an internal standard (0.02 g/L L-2-chlorophenylalanine) and homogenized pulverized for 6 min via cryogenic grinding at-10℃(50Hz). Subsequently, the homogenate underwent ultrasound - aided solvent extraction (5°C, 40 kHz, 30 min) and subsequently incubated at -20°C for 30 min for protein precipitation. The supernatant was then separated by high-speed centrifugation (13,000 × *g*, 4°C, 15 min) for subsequent analysis. The QC samples were prepared by pooling equal volumes (20.0 μL) of the supernatant from each individual sample.

Metabolomic profiling was executed on a UHPLC Q-Exactive HF-X platform (Thermo Scientific, USA). Solute separation utilized an ACQUITY UPLC HSS T3 stationary phase, with 2.0 uL aliquots introduced per run. Binary mobile phases comprised aqueous 0.1% formic acid with 5% acetonitrile (A) and a mixture of acetonitrile/isopropanol/water (47.5: 47.5: 5, v/v/v) containing 0.1% formic acid (B). Following gradient elution, mass spectra were acquired via electrospray ionization in both polarity modes. Key instrumental settings included a mass-to-charge (m/z) scanning window of 70–1050, a 425°C capillary temperature, and a 50.0 V declustering potential. Analytical results represent the mean values derived from ten biological replicates.

The raw mass spectrometry raw datasets underwent preprocessing, incorporating feature detection extraction, alignment, and chromatographic alignment and RT calibration, using Progenesis QI software. Subsequently, qualitative annotation of the metabolites was achieved by searching against public databases (HMDB and METLIN) as well as the Majorbio proprietary database. Statistical analysis was executed within the Majorbio Cloud analytical ecosystem. Specifically, differentially expressed metabolites (DEMs) among the groups were compared usingthe R-based VennDiagram library (v1.7.3) (Chen & Boutros, 2011[14]. Multivariate modeling via partial least squares-discriminant analysis (PLS-DA) models were constructed, and variable importance in projection (VIP) values were calculated utilizing the *ropls* package (version 1.34.0, Etienne Thévenot, CEA, Saclay, France) in R. Furthermore, clustering

analysis and heatmap generation were performed using the *scipy* library in Python to elucidate the overall metabolic profile characteristics.

Transcriptome Analysis of the Sea Buckthorn Branches

Total RNA was extracted from the sea buckthorn tissues, which had been thoroughly ground in liquid nitrogen, using the Trizol reagent method. Specifically, 1 mL of Trizol was added to the sample to guarantee thorough lytic efficiency, followed by incubation under ambient conditions for a 5-minute duration. Centrifugation at 13,000×g for 5 min (4°C) yielded a supernatant that was subsequently transferred and partitioned by the addition of 200uL chloroform. Following thorough mixing and following a 5-minute equilibration under ambient conditions, the resulting blend was centrifuged again under the same conditions for 15 min. An aliquot of roughly 400 μL from the top aqueous layer was meticulously recovered into a fresh microcentrifuge tube and subsequently precipitated by introducing an equivalent volume of ice-cold isopropanol. After precipitating at 25°C for 10 min, the resulting white precipitate was harvested through centrifugal sedimentation (13,000 × g, 10 min). Subsequently, the pellet was resuspended and washed with 1 mL of 75% ethanol. The liquid fraction was discarded following a 5-min spin at 12,000 × g. The resulting pellet was subjected to ambient air-exposure for 3–5 min until visual dryness was achieved, and finally, 20–50 μL of 0.1% DEPC-treated water was added to dissolve the total RNA.

The construction of the strand-specific transcriptome library and subsequent sequencing were conducted by the Shanghai Majorbio Bio-pharm Biotechnology Co., Ltd. (Shanghai, China). Starting with 1 μg of high-quality total RNA as the template, the library was constructed utilizing the Illumina Stranded mRNA Prep Ligation kit. Following Oligo(dT) bead-mediated enrichment and fragmentation of mRNA, double-stranded cDNA was synthesized. Specifically, dUTP was utilized during the assembly of the second strand for downstream identification. The resulting products sequentially underwent end repair, the addition of a single 'A' nucleotide to the 3' ends, and the ligation of sequencing adapters. Following this, the specifically labeled second strand was digested using UDG enzyme to preserve the strand orientation information. The ligated products, approximately 300 bp in size, were selected and subjected to PCR amplification. Upon successful Qubit 4.0-based quantification, the libraries were loaded onto a NovaSeq X plus platform for paired-end sequencing with a read length of 150bp.

After the raw fastq output files were subjected to quality control using *fastp* software, the processed sequencing library was anchored to the reference genome using HISAT2, adopting a hierarchical indexing strategy for efficient mapping, and transcript assembly was accomplished by *StringTie*. Based on the Transcripts Per Million (TPM) method, gene expression abundance was quantified using *RSEM* software. The identification of differentially expressed genes (DEGs) was performed employing *DESeq2* (filtering thresholds: $|\log_2 FC| \geq 1$ and FDR < 0.05). Subsequently, GO and KEGG functional enrichment analyses of the DEGs were conducted using *Goatools* and the *Python scipy* library, respectively, with significance defined by a Bonferroni-corrected *P*-value < 0.05. Furthermore, alternative splicing events

(e.g., exon skipping, intron retention) within the samples were identified and classified utilizing *rMATS* software (version 4.1.2, Xing Lab, University of Pennsylvania, USA).

Statistical Analysis

Bar charts and line graphs were generated utilizing Origin 2021 software. Data points represent the average ± SD/SEM, reflecting the variability and central tendency of the replicates of 4 (targeted metabolomics), 10 (untargeted metabolomics and transcriptomics), or 25 (phenotypic indicators) biological replicates. Statistical comparisons across groups were conducted using one-way analysis of variance (ANOVA), implemented through IBM SPSS Statistics v.27 (IBM Corp., USA). A threshold of $P < 0.05$ was adopted to define statistically significant differences between the mean values. Furthermore, all omics-related visualizations and analyses were executed on the Majorbio Cloud Platform (https://www.majorbio.com/).

Results and Discussion

Analysis of Apparent Traits and Metabolite Accumulation Characteristics in the Sea Buckthorn Fruits Across Different Growth Years

The results revealed that significant differences in color and physical characteristics were exhibited among the sea buckthorn fruits across different tree ages. As illustrated in the Table S1, the length, width, and weight of the fruits were significantly elevated with increasing tree age ($P < 0.05$, n = 25). Furthermore, as demonstrated in the Fig. 1, an upward trend in the quantity of the sea buckthorn fruits was observed as the tree age increased. Concurrently, a higher degree of redness and a lower degree of yellowness were noted. The highest redness value was recorded in the Sea buckthorn fruits with growth for 6 years (6Fyr) (18.54), followed by the Sea buckthorn fruits with growth for 5 years (5Fyr) (18.03), the maximum yellowness was found in the Sea buckthorn fruits with growth for 4 years (4Fyr) (15.92), followed by 5Fyr (13.14). Meanwhile, the highest lightness value was observed in the 5Fyr (21.82) ($P < 0.05$).

The significant increase in redness (a*) and decrease in yellowness (b*) in older fruits likely bolster their sensory appeal and commercial value. Higher redness is reportedly associated with consumer preferences for "nutrient-dense" berries[15]. Consequently, the color profile of 6Fyr fruits aligns better with premium market standards, potentially offering higher economic returns due to superior visual quality and perceived freshness.

Based on the aforementioned phenotypic investigations, a total of 22 bioactive components in the sea buckthorn fruits across different tree ages were initially identified *via* targeted metabolomics (Table 1). Among these, significant ($P < 0.05$) discrepancies became apparent regarding the levels of phenolic compounds, carotenoids, and vitamin C contents. These functional substances were primarily enriched in the KEGG pathways of ko00941, ko00942, and ko00906. Notably, rather than functioning

independently, the *in vivo* accumulation of these metabolites is often comprehensively regulated by upstream pathways, such as phenylpropanoid biosynthesis (ko00940).

Table 1
The Effect of Different Tree Ages on Antioxidant Active Substances in Sea buckthorn Fruits (n = 4).

Item	4Fyr	5Fyr	6Fyr	SEM	*P*
Vitamin C(g/100g)	0.46 ± 0.01a	0.40 ± 0.01b	0.41 ± 0.00b	0.01	<0.001
Procyanidin B4(ng/100mg)	78.19 ± 3.10c	96.59 ± 7.05ab	103.30 ± 7.28a	4.52	0.044
Procyanidin B2(ng/100mg)	24.42 ± 0.81b	29.70 ± 2.07a	29.51 ± 0.94a	1.04	0.041
Pelargonidin(ng/100mg)	0.48 ± 0.10ab	0.45 ± 0.10b	0.76 ± 0.05a	0.06	0.062
Peonidin(ng/100mg)	0.45 ± 0.03b	0.60 ± 0.04a	0.69 ± 0.04a	0.04	0.003
Malvidin(ng/100mg)	0.11 ± 0.02a	0.11 ± 0.02a	0.12 ± 0.01a	0.01	0.735
Delphinidin(ng/100mg)	7.53 ± 1.46a	2.20 ± 0.08b	4.48 ± 0.82ab	0.83	0.012
Cyanidin(ug/100mg)	1.98 ± 0.62a	1.98 ± 0.94a	0.94 ± 0.56b	0.15	<0.001
Petunidin(ug/100mg)	10.56 ± 0.52a	7.32 ± 0.68b	8.73 ± 0.94ab	0.55	0.037
Cyanidin-3-galactoside(ng/100mg)	0.08 ± 0.01a	0.09 ± 0.01a	0.09 ± 0.01a	0.00	0.626
Rutin(ug/100mg)	4.12 ± 0.43a	3.60 ± 0.09b	3.83 ± 0.12b	0.08	0.009
Kaempferol(ng/100mg)	3.86 ± 0.35b	4.31 ± 0.28ab	5.12 ± 0.45a	0.25	0.099
Isorhamnetin(ug/100mg)	0.06 ± 0.00b	0.06 ± 0.00b	0.11 ± 0.01a	0.00	<0.001
Luteolin(ng/100mg)	4.32 ± 0.52b	4.95 ± 0.15b	7.01 ± 0.39a	0.40	0.002
Quercetin(ng/100mg)	15.86 ± 0.26b	17.02 ± 0.87b	23.74 ± 0.14a	1.08	<0.001
Violaxanthin (ug/100mg)	131.23 ± 6.95a	121.80 ± 4.79ab	97.68 ± 9.77b	5.77	0.029
Xanthophyll (mg/100mg)	4.88 ± 0.25a	5.63 ± 0.39a	5.69 ± 0.11a	0.18	0.125
Zeaxanthin (mg/100mg)	4.70 ± 0.25b	5.56 ± 0.28a	6.04 ± 0.15a	0.21	0.009
β-Cryptoxanthin (mg/100mg)	0.57 ± 0.01a	0.65 ± 0.03a	0.62 ± 0.04a	0.02	0.141
α-Carotene (mg/100mg)	0.18 ± 0.14a	0.17 ± 0.02a	0.19 ± 0.02a	0.01	0.866
β-Carotene (mg/100mg)	0.37 ± 0.01b	0.48 ± 0.04a	0.50 ± 0.04a	0.03	0.036

SEM, standard error of the mean. Different lowercase letters (a, b, c) in the same row indicate significant differences at the 0.05 leve

Item	4Fyr	5Fyr	6Fyr	SEM	*P*
Lycopene (mg/100mg)	0.12 ± 0.00b	0.18 ± 0.01a	0.18 ± 0.01a	0.01	0.004
SEM, standard error of the mean. Different lowercase letters (a, b, c) in the same row indicate significant differences at the 0.05 leve					

Furthermore, a significant declining trend in the vitamin C content of the sea buckthorn fruits was observed with the increasing of tree age (n = 5), which aligns with the findings reported by previous research[16]. This phenomenon could be attributed to the combined effects of an attenuated capacity for secondary metabolites synthesis in the older plants, superimposed on a natural deceleration of physiological metabolic rates during fruit maturation[17].

Among the flavonoids, a pronounced dominance in rutin content was observed in a substantially greater concentration ($P < 0.05$) was recorded in the 4Fyr than in the 5Fyr and 6Fyr. This finding was further corroborated by the metabolic pathway map (Fig. 5). Surprisingly, no significant upregulation was detected in the *FG2* (k22772) gene responsible for its regulation. However, the accumulation pattern of its upstream precursor, isoquercitrin, was highly consistent with that of rutin. This phenomenon implies that a low level of mRNA abundance appears capable of preserving the essential the highly efficient conversion of the precursor isoquercitrin into rutin[18]. Conversely, the contents of kaempferol, isorhamnetin, luteolin, and quercetin peaked in the 6Fyr ($P < 0.05$). Notably, the accumulation of kaempferol correlated negatively with its precursor, naringenin, while the FLS gene (k05278) was significantly upregulated. Mechanistically, FLS reportedly acts as a pivotal switch in metabolic branching, competing with dihydroflavonol 4-reductase (DFR) for the shared dihydrokaempferol (DHK) substrate pool[19]. The observed high expression of FLS potentially grants a competitive advantage in substrate recruitment, effectively diverting the metabolic flux toward the flavonol pathway at the expense of anthocyanin synthesis. This shift in dynamic equilibrium suggests a prioritized chemical partitioning that drives the selective accumulation of kaempferol derivatives in older fruits[20, 21].

Procyanidin B_2 and B_4 increased significantly with tree age ($P < 0.05$), likely enhancing the fruit's antioxidant and protein-binding capacities. Mechanistically, the distinctive B-type interflavan linkages in these dimers are reported to expand the molecular surface area and reactive hydroxyl density compared to monomers[22]. This structural evolution is suggested to improve ecological resilience and nutritional functionality by strengthening interactions with biological macromolecules[23, 24].

Comparative analysis of anthocyanidins revealed that 5Fyr contained the lowest delphinidin abundance, which fell significantly below the levels measured in 4Fyr ($P < 0.05$). In the 6Fyr group, a dramatic contraction in cyanidin content was identified, with values appearing highly diminished ($P < 0.001$) compared to the earlier 4Fyr and 5Fyr stages. Similarly, petunidin was significantly less prevalent in the 5Fyr stage than in the 4Fyr ($P < 0.05$). This downward trend of monomeric anthocyanidins is highly consistent with the finding presented in the Fig. 3, where the contents of anthocyanin glycosides, specifically cyanidin 3-rutinoside and peonidin 3-glucoside, were found to increase with tree age. The

shift from monomeric anthocyanidins to glycosides likely drives the observed color intensification. According to chemical equilibrium theory, C3-glycosylation provides steric hindrance that suppresses water-induced nucleophilic attack, thereby stabilizing the red flavylium cations over colorless forms[25, 26]. Furthermore, glycosylation is suggested to mask reactive phenolic groups and form intramolecular hydrogen bonds, which reportedly enhances resistance to thermal and oxidative stress[27]. Such structural modifications may ultimately improve the compounds' bioavailability, consistent with the upgraded quality of fruits from older trees[28–30]. It is suggested that this metabolic strategy is not only beneficial for the accumulation and storage of pigments but also serves as a critical mechanism for regulating the visual color presentation in the fruits of older trees[31, 32].

In sea buckthorn berries, carotenoids serve as the predominant lipophilic fractions possessing significant antioxidant potential. Not only is the visual color of the fruits regulated by these compounds, but they also serve as core secondary metabolic indicators aimed at determining the dietary value and phytochemical composition of sea buckthorn berries[9]. "In the current investigation, seven carotenoids were resolved and quantified from the extracts. Among them, the contents of zeaxanthin, β-carotene, and lycopene increased significantly with tree age ($P < 0.05$), while a significant reduction was observed in violaxanthin ($P < 0.05$). These results suggest that the xanthophyll cycle is activated in older plants, likely through the enzymatic deepoxidation process. Mechanistically, this involves the removal of epoxide groups from violaxanthin to form zeaxanthin[33, 34]. Such a structural transformation is reported to decrease molecular polarity, which could enhance the antioxidant potential and photoprotective efficiency within the thylakoid membrane[35, 36]. Furthermore, the accumulation of these high-stability carotenoids potentially increases the commercial value of older sea buckthorn berries as high-quality sources for eye-health supplements and natural colorants with improved light fastness. Collectively, this shift may represent a strategy to mitigate physiological stress during the aging process[37, 38].

Functional annotation using the KEGG library revealed that the detected metabolites are primarily involved in five core pathways (Table S2). Notable enrichments were observed in the biosynthesis of secondary metabolites and overarching metabolic pathways, alongside specialized branches such as flavonoid and anthocyanin biosynthesis. Within this framework, the global metabolic architecture is anchored by 'metabolic pathways' and 'biosynthesis of secondary metabolites'. Functioning as a pivotal intermediary, the 'flavonoid biosynthesis' sector bifurcates into more specialized terminal branches, specifically encompassing 'anthocyanin biosynthesis' alongside 'flavone and flavonol biosynthesis.” Collectively, the directional focusing of metabolic flux from a global overview toward the targeted synthesis of the flavonoid family is reflected by this hierarchical pathway architecture[39, 40].

Metabolomics Analysis of Sea Buckthorn Fruits

Untargeted metabolomics analysis was performed on sea buckthorn fruits across different growth years. As illustrated in the Figure S1A-1B, a clear spatial separation among the groups was exhibited in the PCA score plots, indicating significant differences in the metabolic profiles among the samples.

Concurrently, the exceptionally high stability and reliability of the detection data were corroborated by these results. In the OPLS-DA models (Figure S1C-1F), a significant separation along the PC1 axis and tight intra-group clustering were demonstrated by the samples, thereby further revealing the dynamic evolutionary characteristics of sea buckthorn fruit metabolites across different years. Additionally, the results of a 200-iteration random permutation test indicated that all R^2 values approached 1.0, and the intercepts of the Q^2 regression lines were negative. The excellent robustness of the models without overfitting was thereby confirmed, laying a reliable foundation for the precise screening of DEMs in subsequent analyses.

According to the differential scatter plots derived from the OPLS-DA models (Figure S1G-1H), a total of 238 significant DEMs were identified between the 6Fyr and 5Fyr, among which 145 were upregulated and 93 were downregulated. In contrast, the number of DEMs between the 5Fyr and 4Fyr increased significantly to 554, with 202 upregulated and 352 downregulated. In previous studies, attention was primarily focused on the differences among metabolites, whereas their specific classifications were largely overlooked[41, 42]. As shown in the classification charts of the annotated secondary metabolites (Figure S1I-1G), a high degree of synergy in the compositional categories of DEMs across different tree age groups was observed in this study. The DEMs were primarily enriched in three major clusters: flavonoids, terpenoids, and phenolic acids and derivatives, with flavonoid glycosides accounting for the highest proportion in both groups (11 types in 6Fyr vs 5Fyr, 22 types in 5Fyr vs 4Fyr). It is indicated by these findings that the glycosylation of flavonoids serves as a core metabolic strategy in sea buckthorn fruits. Such results challenge the notion that sea buckthorn is solely restricted to merely synthesizing flavonoids, but is actively optimizing the storage and accumulation efficiency of these antioxidant substances through enhanced glycosylation to cope with long-term physiological stress[4, 9].

Based on the VIP weight analysis (Fig. 2A – 2B), it was indicated that significant differences in secondary metabolites were exhibited among sea buckthorn fruits across different growth years. The results demonstrated that with the gradual increase in tree age, basic flavonoid monomers, such as dhelwangin, chrysin, and glycitin, were significantly downregulated (VIP > 1). Conversely, flavonoid glycoside derivatives, including 2",6"-di-O-acetylononin, chrysoeriol 7-glucuronide, and spinacetin 3-glucoside, were significantly upregulated (VIP > 1). It is indicated by this phenomenon that basic flavonoid precursors within the sea buckthorn fruits are continuously converted into glycosylated forms with enhanced chemical stability and superior biological activity as the tree ages[43, 44]. Not only is the quality of antioxidant activity elevated by this conversion, but it may also serve as one of the underlying factors driving the alteration in fruit coloration[45].

Furthermore, a significant upregulation was observed in phenolic acids and their coumarin derivatives with increasing tree age, including 2-hydroxy-3-(beta-D-xylopyranosyloxy) benzoic acid, 1-(3,4-dimethoxyphenyl)-1,3-propanediol, isoscopoletin, correolide, 8-hydroxy-3,4,5-trimethyl-6-oxo-4,6-dihydro-3H-isochromene-7-carboxylic acid, (-)-pinoresinol, asarinin, and 4-(4-hydroxyphenyl)-2-butanone *O*-[2-galloyl-6-cinnamoylglucoside] (VIP > 2). It is suggested by these findings that a pronounced overall

activation trend may be exhibited by the phenylpropanoid metabolic pathway. This is laterally corroborated by the pathway map (Fig. 5). As the conduits for transporting nutrients to the fruits, sea buckthorn branches exhibited a conspicuous activation of *PAL* (k10775), *4CL* (k01904), and *CYP73A* (k00487) with advancing age. Consequently, a valid hypothesis is proposed that the branches potentially function as an energy reservoir for the fruits[46–48].

By mapping the differentially expressed metabolites against the KEGG database for pathway annotation (Figure S1K-1L), it was revealed that the differential metabolites among the respective groups were consistently and significantly enriched in pathways such as “Phenylpropanoid biosynthesis” and “ABC transporters.” It is demonstrated by these results that phenylpropanoid metabolism constitutes the core of sea buckthorn quality development with advancing age, thereby verifying the aforementioned hypothesis. Meanwhile, the transmembrane translocation and vacuolar compartmentalization of metabolites, such as flavonoid glycosides, are guaranteed by the synergistic enrichment of ABC transporters[6, 8, 49]. Notably, “Flavonoid biosynthesis” was uniquely annotated in the 5Fyr vs. 4Fyr comparison group. It is reflected by this finding that intense accumulation of flavonoid monomers and compositional remodeling are undergone by sea buckthorn during its mid-growth stage (4Fyr–5Fyr), which is consistent with the findings of Du et al[4]. Conversely, pathways such as “Choline metabolism in cancer” and “Starch and sucrose metabolism” were uniquely annotated in the 6Fyr vs. 5Fyr comparison group. It is indicated that carbohydrate turnover and the supply of glycosyl donors are intensified by sea buckthorn during the 5Fyr–6Fyr period. Consequently, the stability and physiological activity of metabolites are enhanced through glycosylation modifications. This further substantiates the preceding observation that simple precursor substances are converted into highly bioactive glycosylated forms with increasing tree age[2, 50].

Metabolomics and Transcriptomics Analysis of Sea Buckthorn Branches

Untargeted metabolomics analysis revealed a significant spatial separation and tight intra-group clustering among the samples in both the PCA and OPLS-DA models (Figure S2A-2F), thereby elucidating the dynamic evolutionary characteristics of the metabolic profiles in sea buckthorn branches with advancing age. In the 200-iteration random permutation tests, negative intercepts for Q^2 and R^2 values approaching 1.0 were observed, confirming that the models were stable and free of overfitting, which provided a reliable basis for screening DEMs. Furthermore, the reliability of the gene expression data was validated by the PCA score plot derived from the transcriptomics analysis (Figure S3C-3D).

According to the differential scatter plots derived from the OPLS-DA models for the metabolome (Figure S2G-2H), a total of 996 significant DEMs were identified in the 6Byr vs. 5Byr comparison group (521 upregulated and 475 downregulated). In contrast, the number of DEMs in the Sea buckthorn branches after growth for 5 years (5Byr) vs Sea buckthorn branches after growth for 4 years(4Byr) comparison group increased significantly to 1,283 (523 upregulated and 760 downregulated). Concurrently, the

volcano plot results from the transcriptomic analysis demonstrated that 1,829 genes were upregulated and 635 genes were downregulated in the Sea buckthorn branches after growth for 6 years (6Byr) vs. 5Byr comparison. Conversely, in the 5Byr vs 4Byr comparison, 794 genes were upregulated, while an exceptionally high number of genes (1,864) were downregulated (Figure S3E-3F)□.

As illustrated in the Figure S2K-2L, the annotated DEMs in the branches were completely consistent with the classification of secondary metabolites in the fruits. They were primarily enriched in three major clusters: flavonoids, terpenoids, and phenolic acids and derivatives. Notably, flavonoid glycosides accounted for the highest proportion in both comparison groups (40 types in 6Byr vs. 5Byr, 100 types in 5Byr vs. 4Byr), and their absolute quantities were significantly higher than those observed in the sea buckthorn fruits.

The VIP weight analysis (Fig. 2C-2D) indicated a trend in the DEMs of the branches that was diametrically opposed to that observed in the fruits. With increasing tree age, significant downregulations were exhibited by phenolic acids and their coumarin derivatives, flavonoids, and terpenoids. This observation appeared to contradict the results presented in the pathway map (Fig. 5), which demonstrated that relevant genes in the phenylpropanoid pathway were significantly activated with advancing age, leading to the enrichment of downstream metabolites. A plausible explanation for this discrepancy is that the specific metabolites selected within our focused pathways were present at relatively low concentrations in the branches. Consequently, their minimal contribution resulted in their absence from the VIP plots.

The KEGG pathway enrichment analysis (Fig. 2K-2L) revealed that the DEGs between 4Byr and 5Byr were significantly enriched in metabolic pathways, including “Biosynthesis of plant secondary metabolites”, “Biosynthesis of various plant secondary metabolites”, “Biosynthesis of phenylpropanoids”, “Flavonoid biosynthesis”, and “Flavone and flavonol biosynthesis”. This suggests that metabolic activities, particularly the accumulation of bioactive compounds, predominate the transition from 4Byr to 5Byr. In contrast, the comparison between 6Byr and 5Byr highlighted pathways related to nutrient transport and metabolite flux regulation, such as “ABC transporters” and “Protein digestion and absorption”. Furthermore, functional annotation (Fig. 3G-3H) showed that while “Plant hormone signal transduction” and “MAPK signaling pathway - plant” were enriched across all ages, the “Flavone and flavonol biosynthesis” pathway was uniquely enriched in the 4Byr vs 5Byr comparison. These findings indicate that the development of sea buckthorn branches is characterized by distinct physiological stages: an initial phase focused on substance and energy sequestration, followed by a later phase dominated by systemic transport. Consequently, we hypothesize that as tree age increases, branches undergo a functional shift-downregulating primary metabolism while enhancing nutrient translocation toward the fruit.

An integrated weighted gene co-expression network analysis (WGCNA) approach was applied to the DEGs and DEMs from various groups to test the proposed hypothesis, focusing on identifying key modules that link transcriptional shifts to metabolic variations. As depicted in the Figure S4, the DEGs in

the 5Byr vs. 4Byr comparison were clustered into 6 modules. Correlation analysis indicated that the MEblue and MEturquoise modules exhibited a significant positive correlation with the DEMs in the branches, whereas a significant negative correlation was observed for the MEbrown module(Fig. 3). In the 6Byr vs 5Byr comparison, the DEGs were also primarily clustered into 6 modules, among which the MEbrown module was positively correlated with the DEMs, while the MEturquoise module showed a negative correlation(Fig. 4).

Through module visualization network analysis, the top 10 genes from each network map were extracted, and their correlations with the fruit metabolites that increased with advancing tree age were analyzed (Figure S5). The results demonstrated that the fruit metabolites at various stages were influenced by distinct genes. Specifically, fruit metabolites from the 6Fyr vs. 5Fyr group, including 2-hydroxy-3-(beta-D-xylopyranosyloxy) benzoic acid, neostigmine bromide, gentamicin A sulfate, cucumerin B, and manninotriose, exhibited a significant positive correlation with the MEturquoise module of the 6Byr vs. 5Byr branch comparison. Conversely, fruit metabolites from the 5Fyr vs. 4Fyr group, such as 4-(4-hydroxyphenyl)-2-butanone *O*-[2-galloyl-6-cinnamoylglucoside], Ala-Ala-Ile, 2",6"-di-*O*-acetylononin, (-)-pinoresinol, and asarinin, were significantly and positively correlated with the MEbrown module of the 5Byr vs. 4Byr branch comparison. It is further demonstrated by these findings that the accumulation of metabolites in sea buckthorn fruits can be indirectly influenced by gene expression in the branches.

As illustrated in the Fig. 6, by performing KEGG functional annotation on the genes from the 5Byr vs. 4Byr MEbrown and 6Byr vs. 5Byr MEturquoise modules, a “two-stage” dynamic regulatory network, with 5Byr acting as the core turning point, was revealed during the development of sea buckthorn branches from 4Byr to 6Byr. In the first stage (spanning from 4Byr to 5Byr), the branches were primarily characterized by stress response and substrate mobilization. During this period, an explosive upregulation was observed in the expression of the energy sensor *PRKAA* (AMPK) and the senescence/stress signaling factor *PP2C* at the 5Byr stage, indicating that intense nutrient demands from the sink (fruits) and internal senescence signals were perceived by the branches. Driven by these signals, the stress-responsive transcription factor *GBF* was synergistically highly expressed, thereby comprehensively activating the carbohydrate degradation and transformation pathways. Specifically, the expression levels of the starch-degrading enzyme *E3.2.1.2* and the key glycosyl-transforming enzyme *GALE* reached their peaks at 5Byr. Through this process, a massive reservoir of free sugars and glycosyl donors was established for the subsequent glycosylation modification of secondary metabolites. Concurrently, significant downregulations were observed in the expression of *MYBP*, a transcriptional switch governing secondary metabolism synthesis, as well as *TUB* (tubulin) and *PIP5K* (a core factor for vesicle membrane formation), which are responsible for intracellular physical transport. This indicates that energy-consuming metabolic and efflux activities in the branches were attenuated at the 5Byr stage, directing all efforts toward the dismantling and accumulation of the internal substance pool.

In the second stage (spanning from 5Byr to 6Byr), a comprehensive functional remodeling of the branches toward secondary synthesis and targeted transport was executed. Following the completion of

the prior substrate mobilization tasks, significant declines were noted in the energy alarm and sugar transformation genes (*PRKAA*, *E3.2.1.2*, *GALE*) at the 6Byr stage. At this juncture, a true “cross-tissue transport” mode was entered by the branches: a strong rebound in *MYBP* expression was observed, effectively reinitiating the synthesis and glycosylation modification of metabolites (such as flavonoids) by utilizing the abundant glycosyl substrates reserved during the 5Byr stage. Subsequently, the intracellular “logistics transportation system” was reawakened. Synchronous surges were exhibited by both *PIP5K* and *TUB*, driving membrane lipid remodeling to form vesicles and laying down cytoskeletal tracks. Through this mechanism, highly active glycosidic metabolites were directionally pumped out of the cell membrane. This strategy of “staggered execution” in gene expression across the temporal axis perfectly elucidates the highly efficient cross-tissue synergistic mechanism by which the energy allocation in the “source” branches is meticulously regulated during the aging process, thereby driving the formation of quality in the “sink” fruits of sea buckthorn.

The evidence of cross-tissue translocation from branches to fruits introduces a novel perspective for the directional enrichment of functional ingredients. Certain phenolic glycosides synthesized in the branches and subsequently transported to the berries may significantly influence the sensory characteristics - such as astringency and color persistence—during processing. This "source-sink" regulated enrichment strategy suggests that branches are not merely structural supports but active metabolic bio-factories. By manipulating or selecting specific tree ages, the food industry can potentially achieve the directional accumulation of high-value glycosides, thereby enhancing the functional potency and sensory stability of the final products.

Conclusion

In this study, the “source-sink” synergistic mechanism driving the enhancement of fruit quality in sea buckthorn across different tree ages was elucidated based on a multi-omics integrative analysis. It was revealed that a “two-stage” functional remodeling occurred in the branches (the source): the 4Byr–5Byr period was characterized by the accumulation of energy substrates and metabolites, while the 5Byr–6Byr period exhibited a comprehensive shift toward targeted transport. Driven by this translocation, a significant increase in flavonoids was observed in the fruits (the sink), with the metabolic strategy undergoing a profound succession from unstable monomers to highly stable glycosidic compounds. Collectively, this branch-fruit synergistic glycosylation remodeling is identified as the core internal mechanism responsible for the intensified coloration and upgraded quality of fruits from older sea buckthorn trees.

Declarations

AUTHOR INFORMATION

Corresponding Author

Shuai Du – *Key Laboratory of Forage Cultivation, Processing and High Efficient Utilization, Ministry of Agriculture, China, Key Laboratory of Grassland Resources, Ministry of Education, China, College of Grassland Science, Inner Mongolia Agricultural University, Hohhot Inner Mongolia 010019, China*, *orcid.org/0000-0002-2035-0927, E-mail: dushuai_nm@sina.com*

Authors

Lichao He – *Key Laboratory of Forage Cultivation, Processing and High Efficient Utilization, Ministry of Agriculture, China, Key Laboratory of Grassland Resources, Ministry of Education, China, College of Grassland Science, Inner Mongolia Agricultural University, Hohhot Inner Mongolia 010019, China*

Meng Li –*Arxan Forest Industry Co., Ltd., Inner Mongolia Hinggan League, 137801, China*

Xuewei Shi – *Key Laboratory of Forage Cultivation, Processing and High Efficient Utilization, Ministry of Agriculture, China, Key Laboratory of Grassland Resources, Ministry of Education, China, College of Grassland Science, Inner Mongolia Agricultural University, Hohhot Inner Mongolia 010019, China*

Ruhan A – *Key Laboratory of Forage Cultivation, Processing and High Efficient Utilization, Ministry of Agriculture, China, Key Laboratory of Grassland Resources, Ministry of Education, China, College of Grassland Science, Inner Mongolia Agricultural University, Hohhot Inner Mongolia 010019, China*

Gentu Ge – *Key Laboratory of Forage Cultivation, Processing and High Efficient Utilization, Ministry of Agriculture, China, Key Laboratory of Grassland Resources, Ministry of Education, China, College of Grassland Science, Inner Mongolia Agricultural University,* National Center of Technology Innovation for Dairy-Breeding and Production Research Center, *Hohhot Inner Mongolia 010019, China*

Yanzi Xiao – *Grass Industry Collaborative Innovation Research Center, Hulunbuir University, Hulunber Inner Mongolia 021000, China*

Yushan Jia –*Key Laboratory of Forage Cultivation, Processing and High Efficient Utilization, Ministry of Agriculture, China, Key Laboratory of Grassland Resources, Ministry of Education, China, College of Grassland, Resources and Environment, Inner Mongolia Agricultural University,* National Center of Technology Innovation for Dairy-Breeding and Production Research Center, *Hohhot Inner Mongolia 010019, China*

CRediT authorship contribution statement

L. C. H.: Conceptualization, Data curation, Visualization, Validation, Investigation, Writing - original draft. **M. L**: Resources. **X.W. S** and **R.H. A**: Investigation. **G.T. G**, **Y. Z. X** and **Y. S. J:** Supervision. **S D**: Conceptualization, Data curation, Project Administration, Writing - Review & Editing, Funding Acquisition.

FUNDING STATEMENT

This work was supported by the Xing'an League Science and Technology Planning Project (MBJH2025018), Key R&D Transformation Project of Inner Mongolia (2025YFHH0265), National Dairy Technology Innovation Center (2025-JSGG-040).

ACKNOWLEDGEMENTS

We thank the Key Laboratory of Grassland Resources, Ministry of Education, Integrated Key Research Platform for providing the equipment.

AVAIABILITY OF DATA AND MATERIALS

The transcriptome data have been deposited in the NCBI database under the accession number PRJNA1455001. Additional data are available upon reasonable request.

DECLARATION OF COMPETING INTEREST

The authors report no financial or personal conflicts of interest that could be perceived as biasing the research presented in this manuscript.

SUPPORTING INFORMATION

Metabolome analysis of sea buckthorn fruits from different years. (A) PCA Analysis of Fruits from 5-year-old and 6-year-old Sea buckthorn Plants. (B) PCA Analysis of Sea buckthorn Fruits from 4-year-old and 5-year-old Grades. (C) OPLSDA analysis of fruits from 5-year-old and 6-year-old sea buckthorn plants. (D) Replacement test between 5-year-old fruits and 6-year-old fruits. (E) OPLSDA analysis of fruits from 4-year and 5-year-old plants. (F) Replacement test between 4-year-old fruits and 5-year-old fruits. (G) Scatter plot showing differences between fruits of 5-year-old and 6-year-old plants. (H) Scatter plot showing differences between fruits of 4-year-old and 5-year-old plants. (I) Annotation of secondary metabolites among the differential metabolites between 5-year-old and 6-year-old fruits. (J) Annotation of secondary metabolites among differential metabolites between 4-year-old and 5-year-old fruits. (K) KEGG pathway annotations of differential metabolites between 5-year-old and 6-year-old fruits. (L) KEGG pathway annotations of differential metabolites between 4-year-old and 5-year-old fruits(**Figure S1),** Metabolome analysis of sea buckthorn branch from different years. (A) PCA Analysis of branches from 5-year-old and 6-year-old Sea buckthorn Plants. (B) PCA Analysis of Sea buckthorn branches from 4-year-old and 5-year-old Grades. (C) OPLSDA analysis of branches from 5-year-old and 6-year-old sea buckthorn plants. (D) Replacement test between 5-year-old branches and 6-year-old branches. (E) OPLSDA analysis of branches from 4-year and 5-year-old plants. (F) Replacement test between 4-year-old branches and 5-year-old branches. (G) Scatter plot showing differences between branches of 5-year-old and 6-year-old plants. (H) Scatter plot showing differences between branches of 4-year-old and 5-year-old plants. (I) Annotation of secondary metabolites among the differential metabolites between 5-year-old and 6-year-old branches. (J) Annotation of secondary metabolites among differential metabolites between 4-year-old and 5-year-old branches. (K) KEGG pathway annotations of differential metabolites between 5-year-old and 6-year-old branches. (L) KEGG pathway annotations of differential

metabolites between 4-year-old and 5-year-old branches**(Figure S2),** Transcriptome analysis of sea buckthorn branches in different year. (A) Venn diagram analysis of differentially expressed genes between 5-year-old and 6-year-old branches. (B) Venn diagram analysis of differentially expressed genes between 4-year-old and 5-year-old branches. (C) PCA analysis of differentially expressed genes between 5-year-old and 6-year-old branches. (D) PCA analysis of differentially expressed genes between 4-year-old and 5-year-old branches. (E) Heatmap analysis of differentially expressed genes between 5-year-old and 6-year-old branches. (F) Heatmap analysis of differentially expressed genes between 4-year-old and 5-year-old branches. (G) KEGG pathway analysis of differentially expressed genes between 5-year-old and 6-year-old branches. (H) KEGG pathway analysis of differentially expressed genes between 4-year-old and 5-year-old branches**Figure S3,** WGCNA analysis of sea buckthorn branches in different years. (A) WGCNA clustering analysis of genes from 4-year-old and 5-year-old branches. (B) WGCNA clustering analysis of genes from 5-year-old and 6-year-old branches. (C) WGCNA module analysis of genes from 4-year-old and 5-year-old branches. (D) WGCNA module analysis of genes from 5-year-old and 6-year-old branches.**Figure S4,**

Correlation analysis between the top 10 genes in each module of branches and metabolites of fruit growth**Figure S5,** Comparison of physical properties and color indices of *Hippophae rhamnoides* fruits at different tree ages (n=5)**Table S1,** KEGG pathway enrichment analysis of differentially metabolites in *Hippophae rhamnoides* fruits at different tree ages**Table S2,** Standard product information**Table S3,** Gradient concentration information of anthocyanin mixed standard**Table S4,** Gradient concentration information of mixed standards of carotenoids**Table S5.**

References

1. Dolma, T., Uniyal, S. & K. Trees. Livelihoods. Valuing seabuckthorn (*Hippophae rhamnoides* L.) ecosystem services for sustainable development and livelihood: a case study in Ladakh cold desert. *Frontiers in Plant Science.* 2025, *34* (3), 217–229.
2. Wang, Z., Zhao, F., Wei, P., Chai, X., Hou, G. & Meng, Q. J. Phytochemistry, health benefits, and food applications of sea buckthorn (*Hippophae rhamnoides* L.): A comprehensive review. *Frontiers in Nutrition.* 2022, *9*, 1036295.
3. Logesh, R., Prasad, S. R., Chidambaram, K. & Devkota, H. P. Sea buckthorn (*Hippophae rhamnoides* L.) and its potential as functional food: a comprehensive review on its chemistry, pharmacological, and industrial importance. *Phytochemistry Reviews.* 2026, 1–38.
4. Du, W., Ding, J., Lu, S., Wen, X., Hu, J., Ruan, C. J. Identification of the key flavonoid and lipid synthesis proteins in the pulp of two sea buckthorn cultivars at different developmental stages. *BMC plant biology.* 2022, *22* (1), 299.
5. Kalia, R. K. et al. Biotechnological interventions in sea buckthorn (*Hippophae* L.): current status and future prospects. *Trees.* 2011, *25* (4), 559–575.
6. Song, Y., Zhang, G., Chen, N., Zhang, J. & He, C. Metabolomic and transcriptomic analyses provide insights into the flavonoid biosynthesis in sea buckthorn (*Hippophae rhamnoides* L.). *Lwt.* 2023, *187*,

115276.

7. Pawar, R. & Rana, V. S. Manipulation of source-sink relationship in pertinence to better fruit quality and yield in fruit crops: a review. *Agricultural Reviews.* 2019, *40* (3).
8. Yazaki, K. J. ABC transporters involved in the transport of plant secondary metabolites. *FEBS letters.* 2006, *580* (4), 1183–1191.
9. Liang, J., Zhang, G., Song, Y., He, C. & Zhang, J. Targeted metabolome and transcriptome analyses reveal the pigmentation mechanism of Hippophae (sea buckthorn) fruit. *Foods.* 2022, *11* (20), 3278.
10. Gradt, I., Kühn, S., Mörsel, J.-T. & Zvaigzne, G. Chemical composition of sea buckthorn leaves, branches and bark. *In Proceedings of the Latvian Academy of Sciences. Section B. Natural, Exact, and Applied Sciences.*, 2017, Latvian Academy of Sciences: Vol. 71, pp 211–216.
11. Li, T. S. & Schroeder, W. R. Sea buckthorn (*Hippophae rhamnoides* L.): a multipurpose plant. *HortTechnology.* 1996, *6* (4), 370–380.
12. Younis, M., Ismail, T., Esatbeyoglu, T. J. & Research, F. Journal of Agriculture and Food Research. *Journal of Agriculture and Food Research.* 2024, *18*, 101366.
13. Chemists, A. I. Official Method 967.21, ascorbic acid in vitamin preparations and juices. *Official Methods of Analysis of Association of Official Analytical Chemists*. 1995, *2*, 16–17.
14. Chen, H., Boutros, P. C. VennDiagram: a package for the generation of highly-customizable Venn and Euler diagrams in R. *BMC bioinformatics.* 2011, *12* (1), 35.
15. Laaksonen, O., Knaapila, A., Niva, T., Deegan, K. C. & Sandell, M. J. Sensory properties and consumer characteristics contributing to liking of berries. *Food quality and preference.* 2016, *53*, 117–126.
16. Tiitinen, K. M., Yang, B., Haraldsson, G. G., Jonsdottir, S. & Kallio, H. P. Fast analysis of sugars, fruit acids, and vitamin C in sea buckthorn (*Hippophae rhamnoides* L.) varieties. *Journal of Agricultural and Food Chemistry.* 2006, *54* (7), 2508–2513.
17. He, C., Zhang, G., Zhang, J., Zeng, Y. & Liu, J. Integrated analysis of multiomic data reveals the role of the antioxidant network in the quality of sea buckthorn berry. *The FASEB Journal.* 2017, *31* (5), 1929–1938.
18. Niu, T. et al. Combinatorial metabolic engineering of Bacillus subtilis enables the efficient biosynthesis of isoquercitrin from quercetin. *Microbial cell factories.* 2024, *23* (1), 114.
19. Lei, T. et al. Competition between FLS and DFR regulates the distribution of flavonols and proanthocyanidins in Rubus chingii Hu. *Frontiers in Plant Science.* 2023, *14*, 1134993.
20. Jiang, X. et al. Functional characterization of three flavonol synthase genes from Camellia sinensis: Roles in flavonol accumulation. *Plant Science.* 2020, *300*, 110632.
21. Yu, L. et al. Integrated metabolomics and transcriptomics provide key molecular insights into floral Stage-Driven flavonoid pathway in safflower. *International Journal of Molecular Sciences.* 2024, *25* (22), 11903.
22. Heim, K. C. Applications. Natural polyphenol and flavonoid polymers. *Properties, and Applications.* 2012, 23–53.

23. Ogwu, M. C., Izah, S. C. & Joshua, M. Ecological and environmental determinants of phytochemical variability in forest trees. *Microbial cell factories.* 2025, *24* (6), 5109–5137.
24. Reis, M. et al. Unveiling structure–activity relationships of proanthocyanidins with dentin collagen. *Dental Materials.* 2021, *37* (11), 1633–1644.
25. Gamage, G. C. V. & Choo, W. S. Anthocyanins in Fruits. *In Natural Products: Phytochemistry, Botany, Metabolism of Alkaloids, Phenolics and Terpenes*, Springer, 2025, pp 1–15.
26. Wang, Y. et al. Stereoselective C-Glycosylation From Unsaturated Glycosyl Donors. *Chemistry–A European Journal.* 2026, e03599.
27. Rao, M. J. & Zheng, B. The role of polyphenols in abiotic stress tolerance and their antioxidant properties to scavenge reactive oxygen species and free radicals. *Antioxidants.* 2025, *14* (1), 74.
28. Yonekura-Sakakibara, K., Nakayama, T., Yamazaki, M. & Saito, K. Modification and stabilization of anthocyanins. *In Anthocyanins: biosynthesis, functions, and applications*, Springer, 2008, pp 169–190.
29. Stintzing, F. C., Stintzing, A. S., Carle, R., Frei, B. & Wrolstad, R. Color and antioxidant properties of cyanidin-based anthocyanin pigments. *Journal of agricultural and food chemistry.* 2002, *50* (21), 6172–6181.
30. Castillo-Munoz, N., Fernandez-Gonzalez, M., Gomez-Alonso, S., Garcia-Romero, E. & Hermosin-Gutierrez, I. Red-color related phenolic composition of Garnacha Tintorera (*Vitis vinifera* L.) grapes and red wines. *Journal of agricultural and food chemistry.* 2009, *57* (17), 7883–7891.
31. Zhao, C.-L. et al. Stability-increasing effects of anthocyanin glycosyl acylation. *Food chemistry.* 2017, *214*, 119–128.
32. Chen, Y. et al. Updated insights into anthocyanin stability behavior from bases to cases: Why and why not anthocyanins lose during food processing. *Critical Reviews in Food Science and Nutrition.* 2023, *63* (27), 8639–8671.
33. Kuczynska, P., Jemiola-Rzeminska, M. & Strzalka, K. Characterisation of carotenoids involved in the xanthophyll cycle. *In Carotenoids, IntechOpen Rijeka, Croatia*, 2017.
34. Latowski, D., Kuczyńska, P. & Strzałka, K. Xanthophyll cycle–a mechanism protecting plants against oxidative stress. *Redox Report.* 2011, *16* (2), 78–90.
35. Sandmann, G. Antioxidant protection from UV-and light-stress related to carotenoid structures. *Antioxidants.* 2019, *8* (7), 219.
36. Johnson, M. P. et al. Elevated zeaxanthin bound to oligomeric LHCII enhances the resistance of Arabidopsis to photooxidative stress by a lipid-protective, antioxidant mechanism. *Journal of Biological Chemistry.* 2007, *282* (31), 22605–22618.
37. Eskling, M., Arvidsson, P. O. & Åkerlund, H. The xanthophyll cycle, its regulation and components. *Physiologia plantarum.* 1997, *100* (4), 806–816.
38. Xiong, X., Wang, X. & Liao, M. Xanthophyll cycle and its relative enzymes. *Journal of Life Sciences.* 2012, *6* (9), 980.

39. Liu, W. et al. The flavonoid biosynthesis network in plants. *International journal of molecular sciences*. 2021, *22* (23), 12824.
40. Davies, K. M. et al. The evolution of flavonoid biosynthesis. *Philosophical Transactions B*. 2024, *379* (1914), 20230361.
41. Wang, M. et al, Metabolome and transcriptome analyses reveal chlorophyll and anthocyanin metabolism pathway associated with cucumber fruit skin color. *BMC Plant biology*. 2020, *20* (1), 386.
42. Zhang, Q. et al. Transcriptome and metabolome profiling unveil the mechanisms of Ziziphus jujuba Mill. peel coloration. *Food chemistry*. 2020, *312*, 125903.
43. Khodzhaieva, R. S., Gladkov, E. S., Kyrychenko, A. & Roshal, A. Progress and achievements in glycosylation of flavonoids. *Frontiers in Chemistry*. 2021, *9*, 637994.
44. Hao, B., Yang, Z., Liu, H., Liu, Y. & Wang, S. Advances in flavonoid research: sources, biological activities, and developmental prospectives. *Current Issues in Molecular Biology*. 2024, *46* (4), 2884–2925.
45. McClure, J. W. Physiology and functions of flavonoids. *In The flavonoids*, Springer, 1975, pp 970–1055.
46. Sharma, A. et al. Response of phenylpropanoid pathway and the role of polyphenols in plants under abiotic stress. *Molecule*. 2019, *24* (13), 2452.
47. Paul, A., Acharya, K. & Chakraborty, N. Involvement of phenylpropanoid pathway and shikimic acid pathway in environmental stress response. *In Biology and biotechnology of environmental stress tolerance in plants*, Apple Academic Press, 2023, pp 27–66.
48. Li, Y., Xie, Y., Zhang, Y., Fang, X. & Wang, J. Trade-Offs and Partitioning Strategy of Carbon Source-Sink During Fruit Development of Camellia oleifera. *Plants*. 2025, *14* (13), 1920.
49. Biała, W. & Jasiński, M. J. The phenylpropanoid case–it is transport that matters. *Frontiers in Plant Science*. 2018, *9*, 1610.
50. Mu, J.et al. Phenolics from sea buckthorn (*Hippophae rhamnoides* L.) modulate starch digestibility through physicochemical modifications brought about by starch–Phenolic molecular interactions. *Lwt*. 2022, *165*, 113682.

Figures

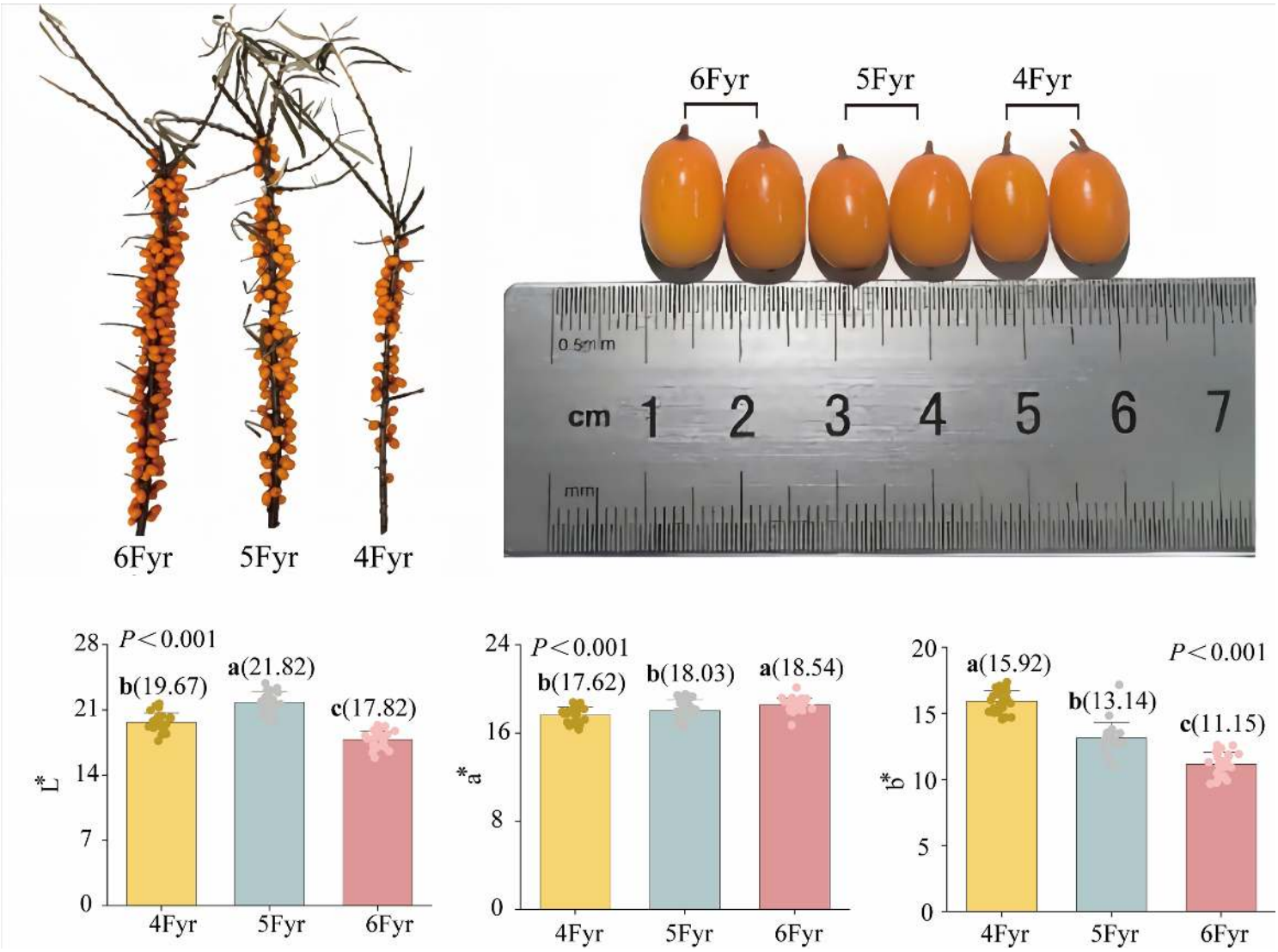

Figure 1

Apparent characteristics and fruit color changes of sea buckthorn in various years. L*, lightness, a*, redness, b*, yellowness. The a, b, c in the bar chart indicated significant differences at the significance level of 0.05.

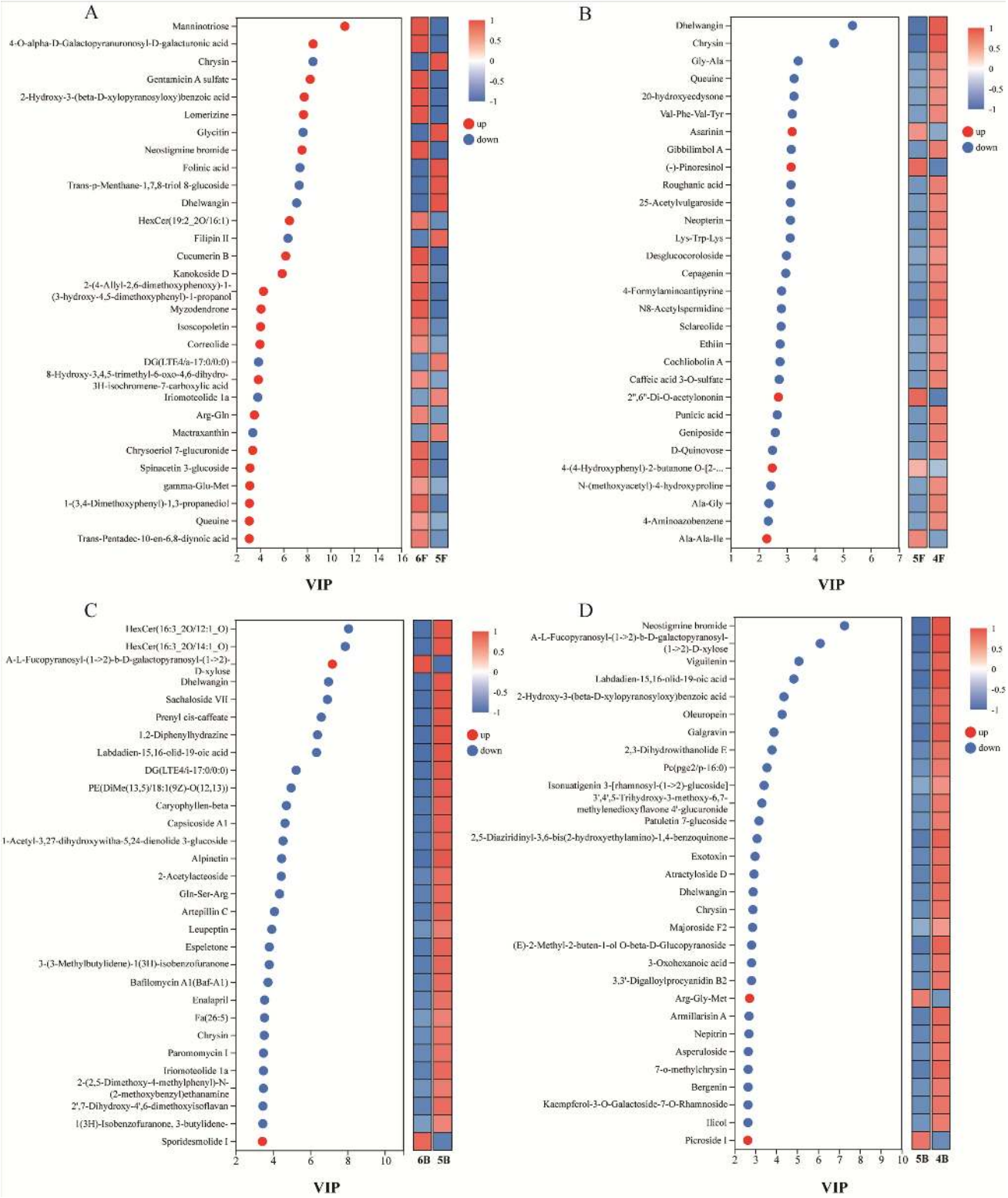

Figure 2

Metabolic remodeling and dynamic evolution in sea buckthorn fruits and branches across different growth years.

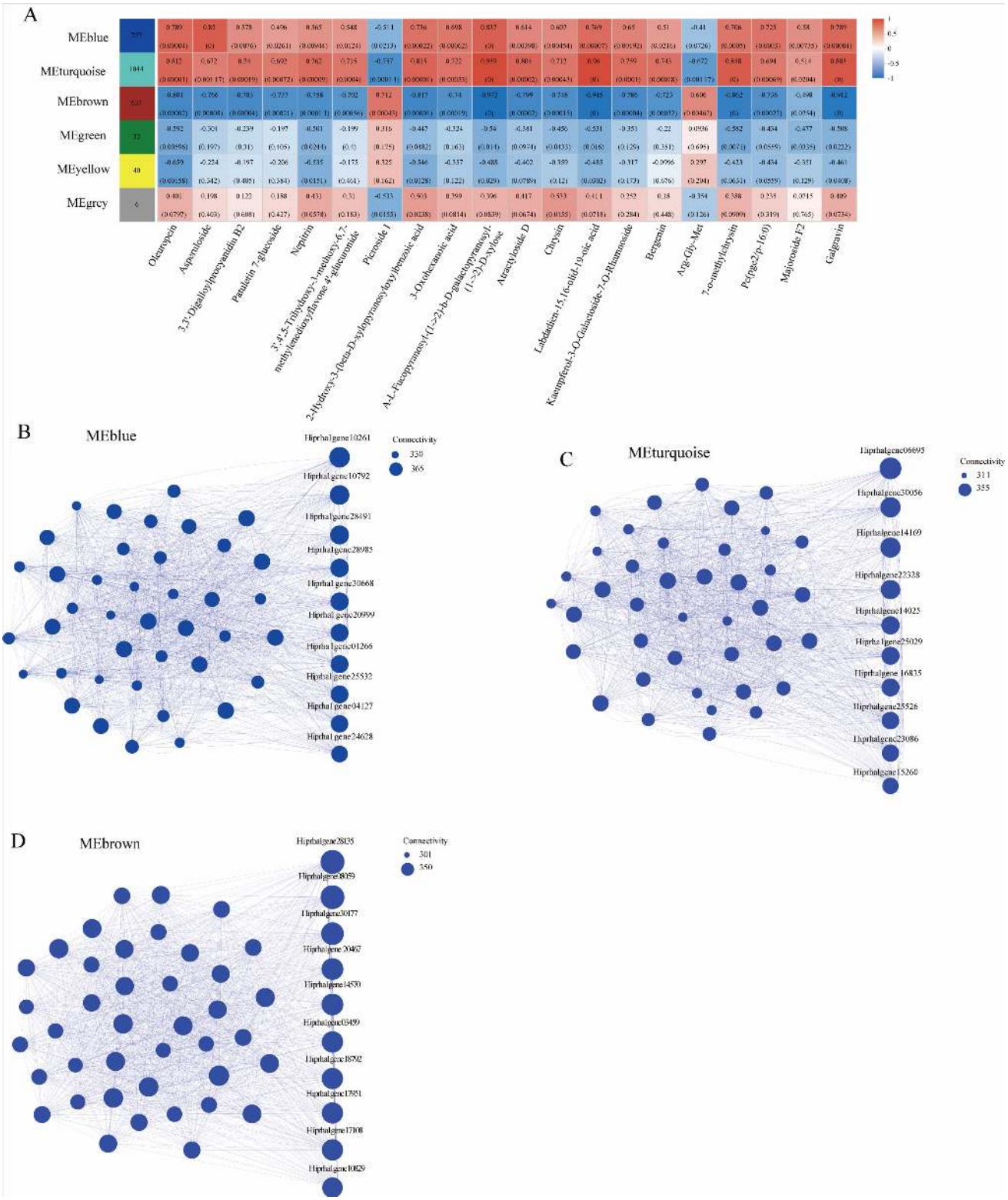

Figure 3

Correlation analysis between the WGCNA analysis module of 4Byr-5Byr branches and metabolites.

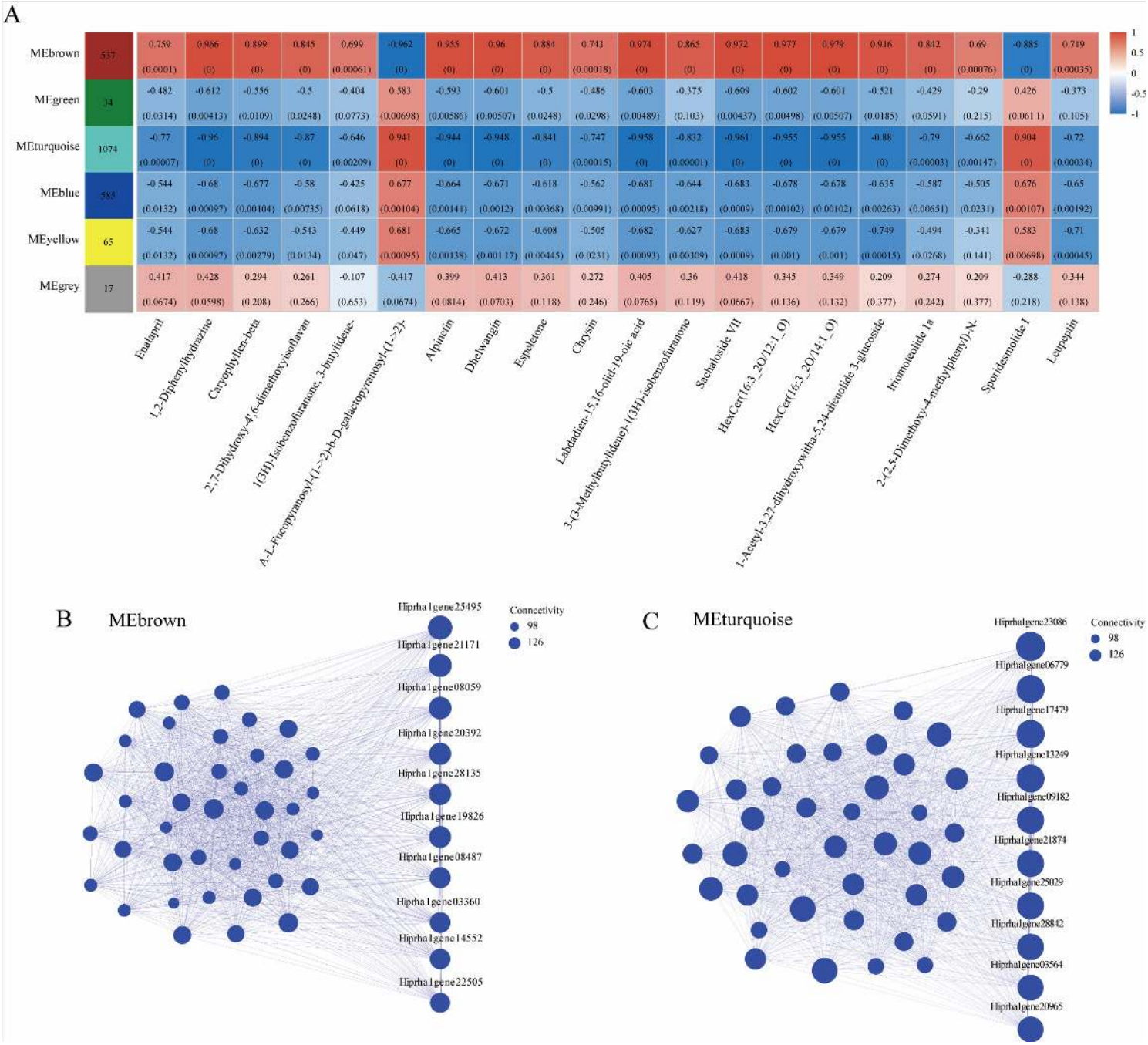

Figure 4

Correlation analysis between the WGCNA analysis module of 5Byr-6Byr branches and metabolites.

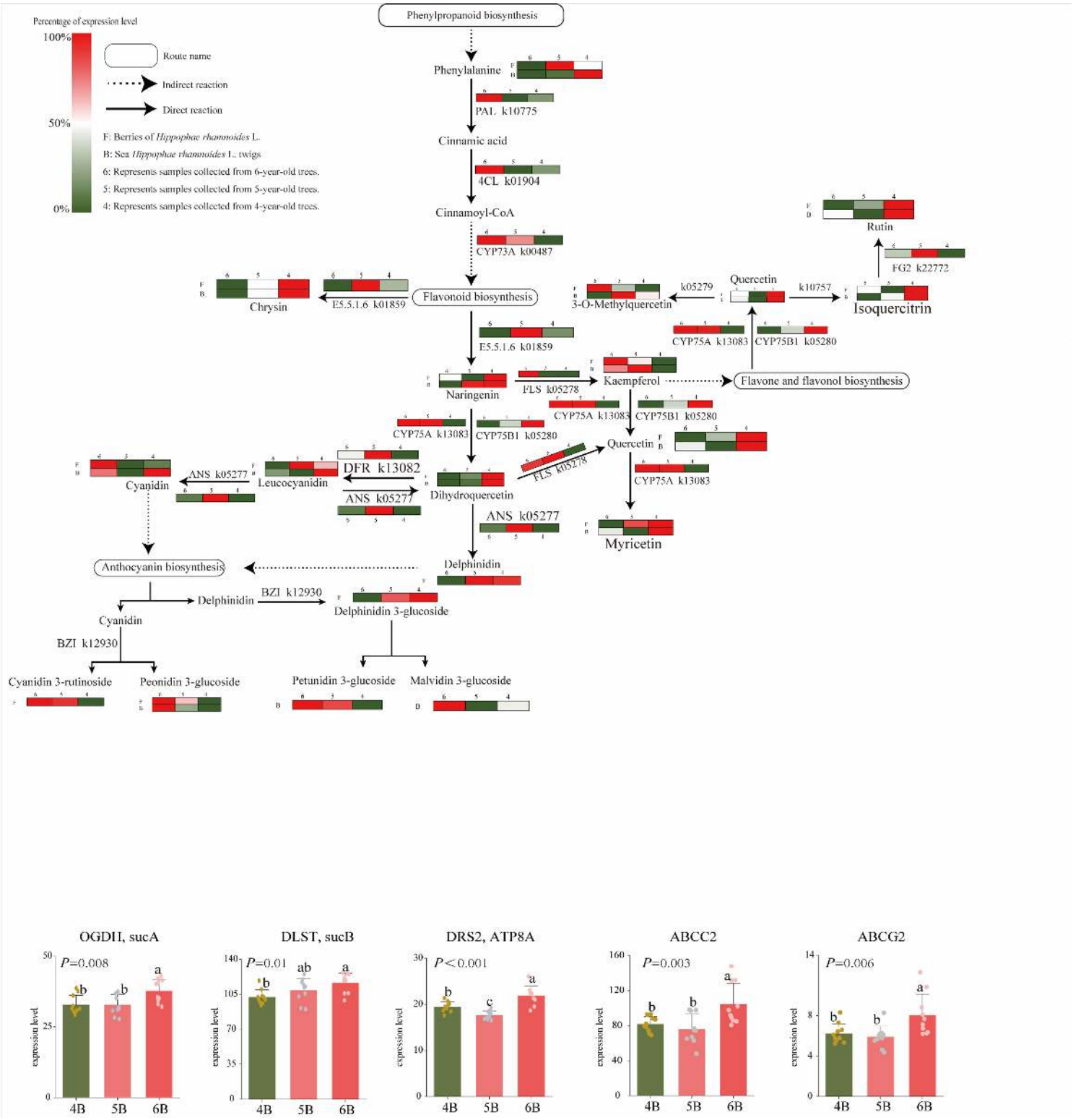

Figure 5

Analysis of metabolic pathways between the branches and fruits.

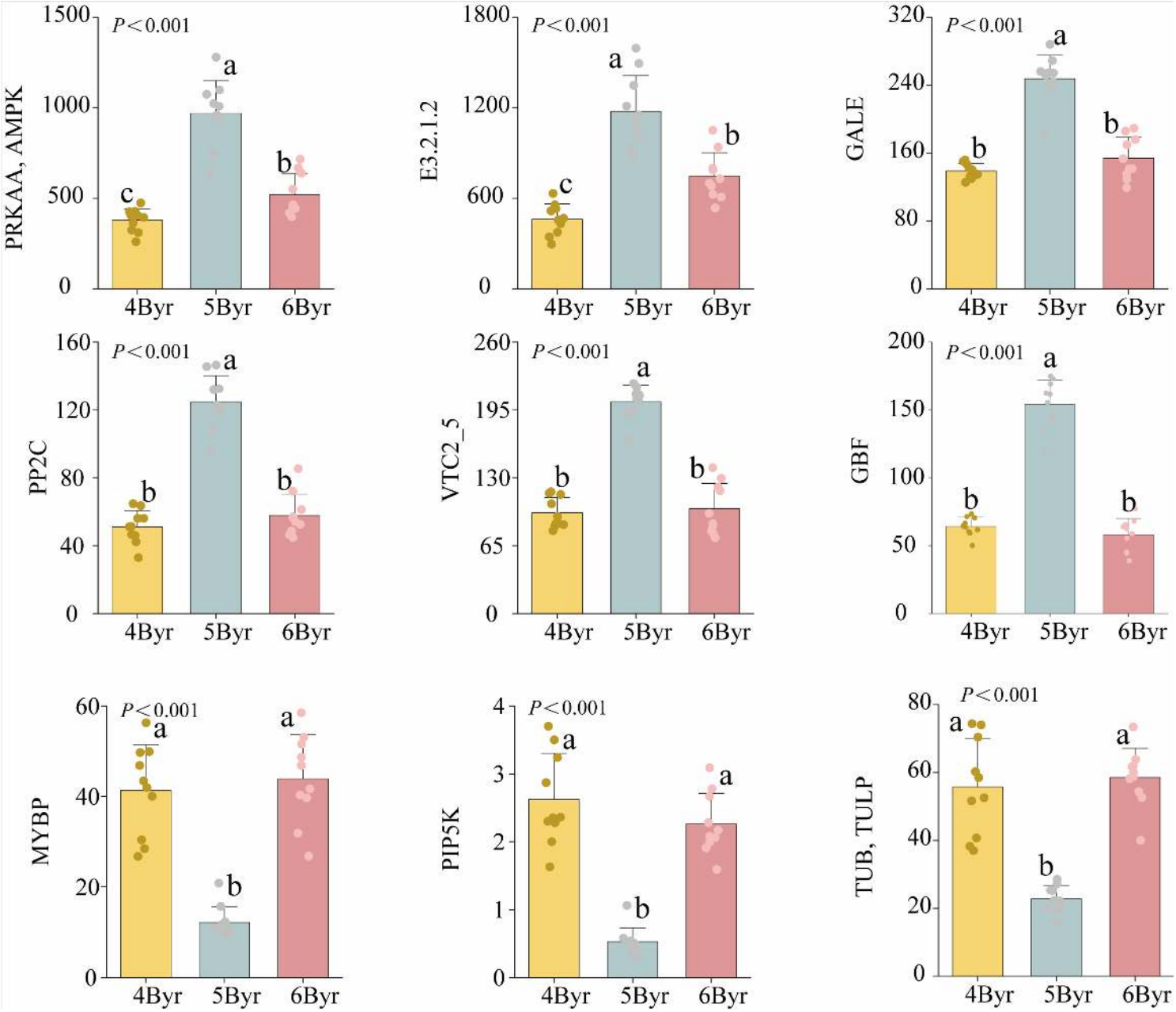

Figure 6

Differential analysis of genes corresponding to two modules of branches from different years. Two modules[1]:5B vs 4B MEbrown, 6B vs 5B MEturquoise. The a, b, c in the bar chart indicated significant differences at the significance level of 0.05.

Supplementary Files

This is a list of supplementary files associated with this preprint. Click to download.

- SupportingInformation.docx